A NON-INVASIVE METHOD TO INVESTIGATE FOOT BONE KINEMATICS

Kilian Rauner[1], Anja Krautter[1], Stefan Lehner[2], Jürgen Mitternacht[1], Veit Senner[1]

Professorship of Sport Equipment and Sport Materials, Technical University of Munich, Germany[1]
Department of Applied Sciences and Mechatronics, Munich University of Applied Sciences, Munich, Germany[2]

The purpose of this study was to investigate whether image correlation photometry in combination with an inverse dynamics foot model is capable of investigating foot bone kinematics. Thus an explorative test setup with one participant was used to acquire the motion data with ARAMIS™ (GOM, Braunschweig, Germany). The motion data enabled a customized inverse dynamics foot model to reproduce the recorded motion and simulate intrinsic movement. Navicular drop was 10.5mm and maximal motion angle did not exceed 23°. The calculated results of navicular drop, range of motion and course of angle over time are promising in comparison to studies using bone pins.

KEY WORDS: Running, mathematical foot model, foot bone kinematics

INTRODUCTION: Running belongs to the top five sport and leisure-time activities amongst adults (Hulteen et al., 2016) and is practiced on many different surfaces and under very different boundary conditions. But not only for optimizing performance but also for the prevention of running injuries, a lot of effort is put into the design of running shoes. A badly designed shoe can harm the athlete due to inadequate support of the foot (Peltz et al., 2014). For systematic optimization of footwear it is essential to fully understand the biomechanics of the foot during running. With this in mind Arndt et al. (2006) postulated that functional footwear can only be designed with precise knowledge about the kinematics of the foot's bones. Bone pins, as used by Arndt et al. (2007) and Wolf et al. (2008), seem to deliver the best results for measuring bone kinematics, but they do raise ethical concerns. Therefore, the purpose of this study was to investigate whether a special digital imaging technique in combination with an inverse dynamics multi-body foot model can produce results of comparable quality.

METHODS: An explorative test setup was designed with one male participant performing one trial of barefoot running on a short running track to acquire the necessary motion data. The participant did not have an abnormal running style or any foot deformations.
To record motion data the digital image correlation system ARAMIS™ (GOM GmbH, Braunschweig, Germany) was used. This system allows to accurately determine 3D-displacement data of entire surfaces based on Triangulation and using stochastic pattern on that surface. Additionally two high-speed stereo cameras recording a ventral close up view of the foot during stance phase were used.
This data was then implemented into a customized fully scalable model of the human foot and ankle (multibody simulation software SIMPACK 9.10, Dassault Systemes Deutschland GmbH, Gilching, Germany). The model represents the 26 bones of the foot, as well as the tibia, the fibula and the femur. The bones' shapes were taken from CT data and their masses and inertia were calculated using the density values provided by Clarys and Marfell-Jones (1986). Further the model contains all passive soft structure as visco-elastic elements, but no muscles. The force element representing the ligaments is a Kelvin body and was developed by Lehner (2007). Ist mechanical properties are taken from Siegler, Block, and Schneck (1988). All degrees of freedom (DOF) of the foot model are presented in Table 1. The orientations of the joint coordinate systems were taken from Schünke (2014).

Table 1
Rotational (R) and translational (T) degrees of freedom of the foot model

Joint	Articular head	Articular cavity	DOF

Talocrural joint	Tibia	Talus	3 R, 1 T
Subtalar joint	Talus	Calcaneus	3 R
Calcaneocuboidal joint	Calcaneus	Cuboid b.	3 R 1 T
Talonavicular joint	Talus	Navicular b.	3 R, 1 T.
Cuneonavicular joint	Navicular B.	Cuneiform b. 1,2,3	3 R, 1 T.
Tarsometatarsal joint	Cuneiform B. 1,Cuboid B.	Metatarsal b. 1, 5	3 R, 2 T
Tarsometatarsal joint	Cuneiform B. 2, 3,Cuboid B.	Metatarsal b. 2, 3, 4	1 R, 2 T

To enable the usage of Aramis motion data to control the motion of the foot model, three major steps had to be undertaken: (1) scaling and positioning of the multibody system (MBS) model to match the data of ARAMIS in size and position, (2) modelling of markers representing selected facets of the ARAMIS mesh, and (3) importing of motion data.
Scaling and positioning was done by using overall foot length and the medial malleolus as anatomical landmark. The facets and movement were modelled using the “Tension-Marker-Bodies” method proposed by Wallrapp, Grund, and Böhm (2005). This means that the surface facets are imported as bodies connected to the inertial system with rheonomic joints. These are connected to individual bones by parallel elastic spring damper force elements. This ensures that the foot skeleton follows the tension marker movement during simulation runtime. The markers presented in Table 2 were the least amount necessary to ensure stable calculation of the model.

Table 2
Modelled tension marker bodies for each bone

Bone	Quantity	Position
Tibia/Fibula	3 x 3	lateral, ventral, medial
Talus	3	lateral, ventral, medial
Calcaneus	2	lateral, medial
Navicular b.	2	medial, superior
Cuboid b.	2	lateral, superior
Cuneiform b. 1	2	medial, superior
Cuneiform b. 2	1	superior
Cuneiform b. 3	1	Superior
Metatarsal b. 1	3	superior distal, superior proximal, medial
Metatarsal b. 2-4	2 each	superior distal, superior proximal
Metatarsal b. 5	3	superior distal, superior proximal, medial

RESULTS: The following three parameters have been chosen to show the possibilities of this new method: (i) range of motion of the talus tibia joint in the sagittal plane, (ii) the angular range of motion of all joints and (iii) the navicular drop.
In Figure 1 the angular displacement of the talus tibia joint is given in the sagittal plane. It is noticeable, that while the simulated angles in the first contact and during toe off phase show minor oscillations, they are quite smooth during mid support. This general characteristic is observable for all joints and planes.

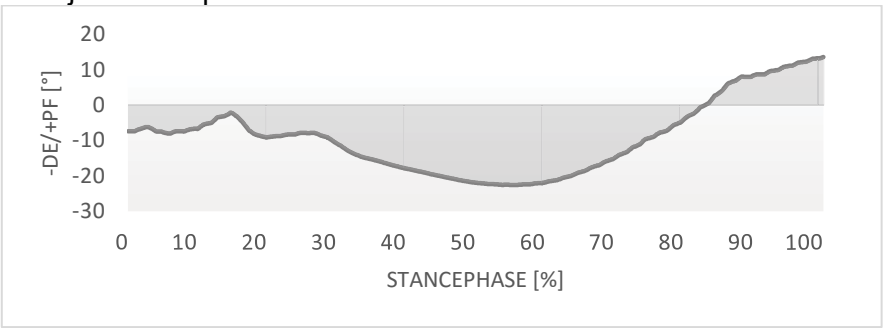

Figure 1: Talus - tibia joint angular displacement during stance phase [%] projected into sagittal plane (+plantar flexion/-dorsal extension)

In Table 3 the angular displacements of eight pairs of foot bones projected into each of the three planes are given. The upper ankle joint, modeled as joint between talus and tibia, shows the highest range of motion.

Table 3
Maximum angular displacement (degrees) between two connecting bones projected in the sagittal plane (SP), frontal plane (FP) and transversal plane (TP).

Plane	Tal-Tib (1)	Calc-Tal (2)	Nav-Tal (3)	Cub-Calc (4)	Cub-Nav (5)	Cun1-Nav (6)	Met1-Cun1 (7)	Met5-Cub (8)
SP	22.54	8.18	6.87	10.02	10.90	10.58	16.40	6.18
FP	9.67	6.57	5.37	12.71	14.94	3.77	8.99	6.58
TP	9.25	2.72	7.94	10.37	10.82	9.20	5.19	6.40

To calculate the navicular drop, the rectangular distance between the navicular bone and a straight line connecting the calcaneus and the metatarsal bone 1 is measured for a reference position, as well as during the whole stance phase. These two values were subtracted and the result is considered the “navicular drop”. Positive values mean lowering of the Navicular bone, while negative values represent a lift in comparison to the reference position.
The maximum navicular drop of 10.57 mm occurs at about 50% of the stance phase. This means that the angle between the calcaneus, the navicular bone, and the metatarsal bone 1 is up to 164°.

DISCUSSION: The minor oscillations seen during foot contact and toe-off in Figure 1 are likely to result out of the measured motion data, since also the motion of the tension markers themselves showed similar behavior. The general course is comparable to data reported by Arndt et al. (2007).
Table 4 compares the calculated ranges of motion using our method to the corresponding values of Arndt et al. (2007) and Wolf et al. (2008), who both used bone pins to determine foot bone kinematics.
11 of our simulated 24 joint angles are within the standard deviation of the values given by these two authors. In additional six cases the values only differ with a maximum 3°. Some of the differences could be due to biological variation, and Arndt and Wolf are also differing to each other as can best be seen in Joint 3. Best Results are achieved for Joint 1 which probably is caused by having at least three tension markers for each bone.

Table 4
Delta values between literature and study results. Positive values indicate that simulated angles are smaller than literature. Deltas marked with * are within SD of the comparison study

Study	Plane	1	2	3	4	5	6	7	8
Arndt et. al	SP	2.16*	-2.48	-0.37*	-2.22	-5.40	-3.48*	-11.50	5.22
(2007)	FP	2.53*	2.33*	8.13	-6.41	-9.44	4.33	-3.69	-1.48
	TP	-0.55*	3.18	0.76*	-3.47	-5.22	-5.10	-0.89*	3.20
Wolf et al.	SP	-	-	-3.97	-2.22*	-5.30	-1.88*	-11.80	5.02
(2008)	FP	-	-	-1.27*	-5.21	-9.34	3.73	-2.19	-1.68*
	TP	-	-	-6.54	-3.37	-5.12	-5.50	-0.99	3.10

The navicular drop is highest with 10.54 mm in mid support phase at approx. 50% normalized time, which is due to shock absorbance during this phase. Our calculated navicular drop corresponds well to literature, results, given by Dicharry et al. (2009) who reported 8.8 $\pm$ 1.8mm at 52% of stance phase. Our simulation results also lie within the ranges reported by Griffin, Miller, Schmitt, and D'Août (2013), and as well in the value range given by Nielsen, Rathleff, Simonsen, and Langberg (2009). Telfer, Woodburn, and Turner (2014) reported angles between calcaneus, navicular bone and metatarsal bone 1 being in the range from 164.1° and 172.3°, which almost corresponds perfectly with our calculated result of 164°.

CONCLUSION: Since not only the calculated navicular drop, as well as the course of angle over time, but also eleven of the foot joint angles show good and six acceptable correspondences to bone-pin-based kinematics, we consider our method as capable to measure 3D-motion-analysis of the foot under dynamic conditions such as running.
In future applications the number of participants, as well as number of cameras should be increased. Further each bone in the MBS model should have at least 3 tension markers to increase orientation quality.

REFERENCES

Arndt, A., Wolf, P., Liu, A., Nester, C., Stacoff, A., Jones, R.,. . . Lundberg, A. (2007). Intrinisic foot kinematics measured in vivo during the stance phase of slow running. *Journal of Biomechanics*. (40), 2672–2678.

Arndt, A., Wolf, P., Nester, C., Liu, A., Jones, R., Howard, D.,. . . Lundberg, A. (2006). Intrinsic foot motion measured in vivo during barefoot running. *Journal of Biomechanics*, *34 (Suppl. 1)*, 182.

Clarys, J. P., & Marfell-Jones, M. J. (1986). Anthropometric Prediction of Component Tissue Masses in the Minor Limb Segments of the Human Body. *Human Biology*, *58*(5), 761–769.

Dicharry, J. M., Franz, J. R., Della Croce, U., Wilder, R. P., Riley, P. O., & Kerrigan, D. C. (2009). Differences in static and dynamic measures in evaluation of talonavicular mobility in gait. *The Journal of orthopaedic and sports physical therapy*, *39*(8), 628–634. doi:10.2519/jospt.2009.2968

Griffin, N. L., Miller, C., Schmitt, D., & D'Août, K. (2013). An investigation of the dynamic relationship between navicular drop and first metatarsophalangeal joint dorsal excursion. *Journal of anatomy*, *222*(6), 598–607. doi:10.1111/joa.12050

Hulteen, R. M., Smith, J. J., Morgan, P. J., Barnett, L. M., Hallal, P. C., Colyvas, K., & Lubans, D. R. (2016). Global participation in sport and leisure-time physical activities: A systematic review and meta-analysis. *Preventive medicine*, *95*, 14–25. doi:10.1016/j.ypmed.2016.11.027

Lehner, S. (2007). *Entwicklung und Validierung biomechanischer Computermodelle und deren Einsatz in der Sportwissenschaft* (Dissertation). Universität Koblenz-Landau, Koblenz-Landau.

Nielsen, R. G., Rathleff, M. S., Simonsen, O. H., & Langberg, H. (2009). Determination of normal values for navicular drop during walking: a new model correcting for foot length and gender. *Journal of foot and ankle research*, *2*, 12. doi:10.1186/1757-1146-2-12

Peltz, C. D., Haladik, J. A., Hoffman, S. E., McDonald, M., Ramo, N. L., Divine, G.,. . . Bey, M. J. (2014). Effects of footwear on three-dimensional tibiotalar and subtalar joint motion during running. *Journal of Biomechanics*, *47*(11), 2647–2653. doi:10.1016/j.jbiomech.2014.05.016

Schünke, M. (2014). *Topografie und Funktion des Bewegungssystems: Funktionelle Anatomie* (2., vollst. überarb. Aufl.). Stuttgart: Georg Thieme.

Siegler, S., Block, J., & Schneck, C. (1988). The mechanical charactersitics of the collateral ligaments of the human ankle joint. *Foot & Ankle International*, *5*(8), 234–242.

Telfer, S., Woodburn, J., & Turner, D. E. (2014). An ultrasound based non-invasive method for the measurement of intrinsic foot kinematics during gait. *Journal of Biomechanics*, *47*(5), 1225–1228. doi:10.1016/j.jbiomech.2013.12.014

Wallrapp, O., Grund, T., & Böhm, H. (2005). Human Motion Analysis and Dynamic Simulation of Rowing. In J. Goicolea, J. Cuadrado, & J. Garcia Orden (Eds.), *Proceedings of MULTIBODY DYNAMICS 2005, ECCOMAS Thematic Conference.* Madrid, Spain.

Wolf, P., Stacoff, A., Liu, A., Nester, C., Arndt, A., Lundberg, A., & Stuessi, E. (2008). Functional units of the human foot. *Gait & Posture*, *28*(3), 434–441. doi:10.1016/j.gaitpost.2008.02.004

Acknowledgment
The authors would like to thank adidas AG (Herzogenaurach, Germany) for providing ARAMIS and their biomechanics lab for the measurements.